

# **Use of Accelerated Loading Equipment for Fatigue Characterization of Hot Mix Asphalt in the Laboratory**

**A Dissertation submitted for  
partial fulfillment of the requirements for the Degree of  
Doctor of Philosophy  
in  
Civil Engineering**

**by**

**Sudip Bhattacharjee  
Department of Civil and Environmental Engineering  
Worcester Polytechnic Institute  
100 Institute Road, Worcester, MA, 01609, USA**

**January 2005**

## ACKNOWLEDGEMENT

I thank my advisor Dr. Rajib B. Mallick for giving me the opportunity to work with the state-of-the-art testing and computational facilities in pavement research laboratory in the department of civil and environmental engineering at Worcester Polytechnic Institute. He gave me the opportunity to work in many externally funded projects, which increased my knowledge of pavement engineering considerably. Without his advice, guidance and financial support this study would not have been possible.

During my doctoral program I had the privilege to work with Professor Frederick Hugo of University of Stellenbosch, South Africa. His advice on many technical matters of my work not only increased my knowledge considerably in the area of accelerated pavement testing, but also helped me to find new directions of research. I also thank Johan Muller for helping us to solve many technical problems we faced while running MMLS3.

I would also like to thank the members of my dissertation committee, Dr. Malcolm H. Ray and Dr. Animesh Das, for providing valuable comments to my work, which helped me to bring the dissertation to the final form.

Special thanks also go to my friend Jonathon Scott Gould for helping me running the tests in the laboratory.

I also thank my following colleagues for their help in my study: Sean O'Brian, Justin Yong, Don Pellegrino, Arthur F. Bealand and Yamini V. Nanagiri.

I thankfully acknowledge the financial support provided by Maine Department of Transportation in this study.

I would like to thank my friend Joe for making my time spent at the department a memorable one. I would also like to specially thank my wife Jayati for giving me encouragement and moral support to my work throughout my doctoral study.

## **ABSTRACT**

In this dissertation, studies of accelerated pavement testing have been discussed and the relative advantage of using the Model Mobile Load Simulator 3 (MMLS3) has been illustrated. A test protocol of using MMLS3 as a fatigue characterization tool has been proposed and validated by testing several Hot Mix Asphalt slabs. Data acquisition was performed with strain gauges placed in different directions under slabs in controlled environmental condition. Analysis of data showed the effect of wheel load on fatigue behavior of pavement in terms of strain history response, cracking and reduction of modulus. Performance curves showing relation between initial strain and failure loads were developed and were compared with the performance curves obtained from standard method. It has been shown that rutting related excessive permanent strain due to movement of particles under wheel path can affect fatigue performance of Hot Mix Asphalt pavement. Method of estimation of time dependent strain has also been developed to predict observed strain.

# Table of Contents

<b>Chapter</b>	<b>Title</b>	<b>Page No</b>
	List of Figures	iv
	List of Tables	vi
1	Introduction	1
2	Objectives	3
3	Scope	4
4	Literature Review	6
5	Need For the Present Study	28
6	Equipment and Materials	33
7	Test Methods Used In This Study Other Than APT	38
8	Test and Analysis Plan	44
9	Development of Model Pavement and Test Protocol Using MMLS3	48
10	Test Results and Analysis	66
11	Contribution to Knowledge	114
12	Conclusions and Recommendations	115
13	Bibliography	117

## List of Figures

Figure No	Title	Page No
5.1	Effect of HMA elastic modulus on the parameter 'A'	30
6.1	A longitudinal cross section of loading equipment of MMLS3	34
6.2	Compaction of HMA in the mold using vibratory compactor	35
6.3	Typical cross section of model pavement	35
7.1	Indirect Tensile Test	39
7.2	Resilient Modulus Test Setup	41
7.3	Periodic Loading for Resilient Modulus Test	42
8.1	Test and Analysis Plan	45
8.2	Positions of Strain Gauges and Thermocouples	46
9.1	Schematic diagram of steps	48
9.2	Leveled surface of sand	50
9.3	Compaction platform with neoprene layer for trial slab	51
9.4	Lowering the steel plate	51
9.5	Steel compaction platform with wooden frame	52
9.6	Aluminum sheets to be placed on top of the steel plate	53
9.7	Aluminum sheets were peeled off from bottom of test slab	53
9.8	Heaters on top of compaction platform	55
9.9	Silicon spray on top of compaction platform	56
9.10	Typical spreadsheet for compaction of mix	56
9.11	Compaction of HMA in the mold	57
9.12	PQI readings are being taken on top of the compacted slab	58
9.13	Cutting of slab after cooling by dry ice (note dry ice bags on top of adjacent slabs)	59
9.14	Separating slabs	60
9.15	Sliding slab onto plywood board	60
9.16	Removing plywood board	61
9.17	Cutting grooves for strain gauges and thermocouples	63
9.18	Attaching strain gauges	63
9.19	Complete setup before starting loading	65
10.1	(a) Transverse strain history	67
	(b) Longitudinal strain history	67
10.2	(a) Permanent strain history for Slab J. SG4,6,8= longitudinal	68
	(b) Resilient strain history for Slab J. SG4,6,8= longitudinal	68
	(c) Permanent strain history for Slab K. SG1,3,5= longitudinal	69
	(d) Resilient strain history for Slab K. SG1,3,5= longitudinal	69
	(e) Permanent strain history for Slab L. SG2,4,6,8= longitudinal	70
	(f) Resilient strain history for Slab L. SG2,4,6,8= longitudinal	70
	(g) Permanent strain history for Slab N. SG1,4,6=longitudinal	71
	(h) Resilient strain history for Slab N. SG1,4,6=longitudinal	71
10.3	Schematic diagram of typical resilient strain history	72

<b>Figure No</b>	<b>Title</b>	<b>Page No</b>
10.4	(a) Variation of temperature for Slab J	73
10.4	(b) Variation of temperature for Slab K	74
10.4	(c) Variation of temperature for Slab L	74
10.4	(d) Variation of temperature for Slab N	75
10.5	(a) Photograph of cracks formed on top of HMA test slab	81
	(b) Increase in crack length due to traffic	81
10.6	Failure load versus initial strain relations	83
10.7	Difference between MMLS3 curve and AI curve	85
10.8	(a) Rut depth versus load number	87
	(b) Typical rutted surface of test slab	87
	(c) Typical cross sectional view of test slab before and after traffic	88
10.9	LVDT positions (Slab Q) along with acquisition system	90
10.10	(a) Average strain from SG for Slab Q	91
	(b) Average LVDT strain from Slab Q	91
10.11	(a) Resilient strain from strain gauge for Slab Q	92
	(b) Resilient strain from LVDT for Slab Q	92
10.12	Finite element mesh model of MMLS3 model pavement	98
10.13	(a) Longitudinal strain contour at top of HMA slab	99
10.13	(b) Longitudinal strain contour at bottom of HMA slab	99
10.14	Direction of principal strains under model pavement	100
10.15	Periodic loading of MMLS3	102
10.16	Slab dimensions and relative positions of strain gauges and load	102
10.17	Calculated response at transverse strain gauge due to one pass	109
10.18	Calculated response at longitudinal strain gauge due to one pass	110

## List of Tables

<b>Table No</b>	<b>Title</b>	<b>Page No</b>
6.1	Gradation of aggregates used	37
9.1	Calculation of Young's modulus of sand (using Geogauge)	49
10.1	Initial strains, failure load and test temperatures for test slabs	76
10.2	Average strains for test slabs	78
10.3	Change of Resilient Modulus Due to MMLS3 Loading	80
10.4	Initial and Final Air Voids in Different Slabs	93
10.5	Typical Horizontal Strain Distribution Along Length Due to Rutting	94
10.6	Effect of temperature gradient on strain	96

# Chapter 1

## INTRODUCTION

Researchers have been using different types of equipment and procedures to characterize Hot Mix Asphalt (HMA) – the reliability of results has always been dependent on the level of sophistication and the closeness of the test conditions to field conditions. Use of pneumatic or hydraulic powered equipment in different modes is very common in the laboratory. In most cases, samples used in such tests are cylindrical or beam samples with relatively small dimensions, and most tests consist of short term loading. Such tests therefore do not give us long term performance indications. Because of practical limitations of using such tests, pavement engineers have resorted to “full-scale” testing – using test tracks, for example. While there is no doubt that full scale testing offers significant advantages over laboratory “small scale” testing, such full scale tests are very costly, time consuming and need a tremendous amount of coordination among partnering agencies. On the other hand, it is quite true that without proper material characterization, accurate prediction of mix and structural performance is impossible – and the prediction will always be as good as the inputs from material characterization are. Therefore, there is a need to determine whether a laboratory scaled model and accelerated loading and testing procedure can be used effectively for material characterization.

There had been several small scaled wheel tracking tests performed in several parts of the world to investigate the behavior of HMA slabs under repeated loading and environmental conditions. Although most of the tests made an attempt to replicate field conditions in the laboratory, proper replication was not achieved because responses observed in test pavements in terms of stress/strain distribution were not similar to the responses observed in real pavements. The loading was bi-directional, therefore resulting strain signals at the end of the slabs had different periods than those at the middle of the slabs. Therefore, results obtained from those tests were only useful in the conditions under which the tests were performed in the laboratory; no prediction of actual pavement

performance was possible. Moreover, almost all of the studies fell short of developing a proper acceptable test protocol under which the tests should be performed.

The advent of one tenth scale Model Mobile Load Simulator (MMLS) during early nineteen nineties and subsequent development of its one third scale counterpart (MMLS3) made it possible to investigate the fatigue behavior in laboratory in more realistic manner. MMLS3 uses an accelerated loading equipment to apply repeated unidirectional loading on a scaled layered pavement structure under controlled environmental conditions. This equipment is built to maintain a scaling factor between model pavement and prototype and thus the results obtained with this equipment is applicable more closely to field conditions with less uncertainties compared to other conventional fatigue test methods.

The majority of MMLS3 studies have focused on evaluation of rutting performance and moisture damage. Relatively little has thus far been done on characterization of pavement materials and layers in the laboratory. This dissertation presents the results of a fatigue test program with the MMLS3 with the purpose of establishing test protocols and developing fatigue characteristic curves of HMA under conditions similar to field conditions. Several fatigue tests were conducted on instrumented model HMA pavement slabs. The feasibility of test procedure was validated through analysis of data and modeling of test pavement. The total dissertation has been divided into 12 chapters. The objectives and scope are presented in **Chapter 2** and **3** respectively. A detailed review of existing studies on accelerated pavement testing has been presented in **Chapter 4** and the need for the present study has been discussed in **Chapter 5**. **Chapter 6** contains the descriptions of equipment and materials used in this study and the various test methods other than accelerated pavement testing used in this study are discussed in **Chapter 7**. The overall test and analysis plan is discussed in **Chapter 8** and the development of the new fatigue testing protocol using the MMLS3 is discussed in detail in **Chapter 9**. The test results and analysis of test results are presented in **Chapter 10**. The contributions of this study to the knowledge of accelerated pavement testing are mentioned in **Chapter 11** and the conclusions and recommendations are discussed in **Chapter 12**. A list of references used is provided at the end of the dissertation.

## **Chapter 2**

### **OBJECTIVES**

The objectives of the study reported in this dissertation were to evaluate the MMLS3 and develop appropriate testing and analysis protocols for using MMLS3 equipment for fatigue characterization of HMA in the laboratory. In particular, this study focused on the following objectives:

- (1) Develop fatigue testing and analysis protocol,
- (2) Develop fatigue related material characterization using accelerated loading equipment,
- (3) Investigate effect of different factors (such as rutting) on fatigue properties of HMA using accelerated loading equipment and
- (4) Modeling of pavement under repeated loading

## Chapter 3

### SCOPE

The scope of the study included the following:

#### **(1) Literature review**

A detailed review of the literature on accelerated pavement testing was performed and is presented in **Chapter 4**. Advantages and disadvantages of several full-scale tests are discussed. Results from studies of several small-scale wheel-tracking devices have been discussed in **Chapter 4** along with their usefulness as tools for material characterization of HMA. The literature on tests with scaled pavement testing equipment is presented and the need for the present study is established in **Chapter 5**.

#### **(2) Modeling of HMA pavement**

Modeling of HMA pavements using the finite element method and analytical method is presented in **Chapter 10**. This was done in view of estimating strain under moving load at any point in time.

#### **(3) Experiments and development of test protocol**

A detailed test protocol and plan for tests with scaled model HMA pavement is presented in **Chapter 9**. A step by step procedure for constructing a scaled model pavement, loading, instrumentation and data acquisition is presented.

#### **(4) Tests**

Results of several tests on instrumented scaled model pavement constructed according to the protocol and loaded with MMLS3 are reported in **Chapter 10**.

#### **(5) Analysis of results**

Analysis of data acquired during each test provided the understanding of behavior of HMA under moving load, especially the fatigue behavior and effect of rutting. Characteristic curves of the mix were developed and the usefulness of MMLS3 as a fatigue characterization tool was established. This is discussed in **Chapter 10**.

#### **(6) Conclusions and recommendations**

Based on the study performed on scaled pavement model, several conclusions were made on the use of MMLS3 as a fatigue characterization tool in the laboratory and recommendations for the use of this equipment were developed. These are presented in **Chapter 12**.

## Chapter 4

# LITERATURE REVIEW ON APT

### 4.1 Introduction

Accelerated pavement testing has been one of the primary methods of testing pavement performance for a long period of time. Several types of accelerated testing facilities have been developed throughout the world. All of the facilities can be categorized into three main types:

1. *Large scale or full-scale pavement test facilities:* The full-scale facilities include Heavy Vehicle Simulators (HVS), which are full-scale loading equipment and apply a load and tire pressure equal to the loading experienced by pavement in field. The load and tire pressures are adjustable to apply a wide range of loading encountered in field. A test section or several test sections are prepared using one or several mixes to be tested and the full-scale load is applied continuously until a particular test section of the pavement fails. The test sections are generally instrumented with strain gauges and pressure sensors and continuous data acquisition is performed. The data acquired are later analyzed for determination of pavement performance, such as fatigue and rutting characteristics. A few examples of these types of facilities are the Texas Mobile Load Simulator (TxMLS) of Texas A&M, full scale testing facility at National Center for Asphalt Technology, Auburn, Alabama, WesTrack at Nevada by Federal Highway Administration and LINTRACK at Technical University of Delft, Netherlands.
2. *Small- scale pavement test facilities:* This type of accelerated loading facilities include small-scale wheel tracking devices, which apply an accelerated load on a scaled down pavement structure. The scaled down pavement structure is prepared

considering a particular dimensional scaling factor on full scaled pavement. The load and tire pressure are also scaled down. The test pavements are instrumented and data are analyzed for pavement characterization. The example of this type of facility is the one-third scale Model Mobile Load Simulator (MMLS3).

3. *Accelerated pavement testing on samples prepared in the laboratory*: There are several testing equipment available, which apply accelerated loading on a sample of HMA prepared in the laboratory. Examples of this type are beam fatigue tests, indirect tensile fatigue tests, rut tests using Asphalt Pavement Analyzer (APA), etc.

Metcalf [1] presented a discussion on the Accelerated Pavement Test (APT) facilities available on or before 1998. Objective of the study was to present the state of the art APT testing methods and applications. The scope of the study included the followings:

1. The study began with the explanation of the definition of APT.
2. A brief historical review of the APT has been presented which included listing of test roads and test tracks used.
3. A discussion on the APT facilities available on or before 1998 was presented with the emphasis on different loading configuration, pavement configuration, instrumentation, capabilities and limitations.
4. Application of APT to research on the stress/strain modeling, deflection/deformation modeling, fatigue modeling and material and layer equivalencies.

The main conclusion drawn from the study mentioned above was that the APT has an enormous potential on the future pavement design and performance analysis and must be pursued for various studies including studies on economic benefits arising out of the testing.

A large amount of data has been extracted from APT studies [2] conducted around the world and analyzed for modeling stress/strain, deformation (rutting), surface deflection, fatigue and layer equivalencies. The most frequently tested parameters are

rutting and fatigue cracking properties of the pavement material. The test sections are prepared with different mixes and are loaded with different magnitude of load and speed to determine the performance of the mixes. Numerous APT studies have been reported. In addition to this study, the conference on APT in Reno, Nevada, USA in 1999, provided an opportunity for international overview of the field of accelerated pavement testing [3]. In the following section, a review of several important studies on full scaled APT performed in different parts of the world is presented.

#### **4.2 Full-Scale APT**

The research performed by Groenendijk *et. al.* [4] and Groenendijk [5] have a particular bearing on this research. The performance of 150 mm and 70 mm thick HMA pavements in field was investigated using LINTRACK [4]. The device consists of a truck wheel (single or dual), which can move bi-directional with a maximum speed of 20 kmph underneath a steel gantry spanning 20 m. The wheel load was adjustable between 15 kN to 100 kN. Both rutting and fatigue performance of test pavements were investigated with the use of five (5) transverse and five (5) longitudinal strain gauges as well as pressure cells and thermocouples. The fatigue life of pavement was compared with predicted values from four-point bending tests (using shift factors) and observed values from strain readings. Among other factors, the effect of rest periods on shift factors was considered.

The behavior of strain gauges under the wheel track of LINTRACK was reported by Groenendijk [5]. Both longitudinal and transverse strain gauges were placed radially along the wheel path and signals were studied. The measured strain distribution showed that magnitude of transverse strains was higher than longitudinal strains. Moreover, transverse strain gauges showed effect of permanent strain accumulation in much higher magnitude than in longitudinal directions. In his study, it was pointed out that temperature corrections are also necessary to account for strains arising from temperature variation (-5°C to 40°C) during the test. To achieve this, temperature correction factors were applied to observed strains at LINTRACK loading to convert the strains to values at reference temperature. Percentage of cracks was monitored by using digitized photograph of wheel track. Pavement life was also observed in terms of visible cracking, HMA

stiffness and rut depth. The fatigue criterion chosen for the study was the deterioration of HMA stiffness to half of its original values as determined from FWD study. Three types of cracking were observed: transverse, longitudinal and alligator. For LINTRACK, maximum rut depth of 18 mm was chosen as failure criterion based on Dutch design standards, while three different cracking criteria were used: class I (small cracking – no influence on traffic), class II (moderate – detrimental effect on riding comfort) and class III (potential danger to traffic safety). It was shown in the study that non-transient or permanent strains in transverse strain gauges were dependent on previous loading, peak strain level, temperature and orientation and locations of strain gauges. On the other hand, very little of non-transient strain was observed in longitudinal direction because of tension-compression effect in that direction. Due to variations in loadings, the strains were converted to relative strain factor for each strain gauge (i.e., relative to a strain due to a standard wheel load at that strain gauge). The BISAR software was used to calculate strain factors and was compared with the measured strain factors. The comparison showed that these two factors did not match in many situations, and it was concluded that the reason for the mismatch was the non-circular, non-uniform contact stress distribution. Fatigue life was predicted based on four point bending tests and was compared with observed life. In many test sections, predicted life matched with observed life based on measured strain, but predicted life was less than the observed life based on back calculated stiffness of HMA. As mentioned earlier, it was also pointed out that, rest period in tests increased fatigue life in many situations.

Molenaar *et. al.* [6] presented several performance models based on results obtained from the LINTRACK study. The probability of failure was modeled as Weibull distribution with data from visual crack percentages in the wheel path:  $F_w(t) = C*[1-\exp(-n/\mu)^\beta]$ , where, C is a correction factor depending on the test section, n is the number of load applications,  $\mu$  is the number of load applications when 63 percent of area is damaged and  $\beta$  is the curvature parameter. The permanent deformation model was developed as:  $S/S_T=(n/N)^b$ , where, S is the rut depth (mm) at any time t,  $S_T$  is the final rut depth at the termination of test (18 mm), n is the applied number of load, N is the number of load application producing 18 mm rut and b is a constant equal to 0.41. Surface curvature was modeled at any time as:  $SCI=d_0-d_x$ , where, SCI,  $d_0$  and  $d_x$  are surface

curvature index, maximum deflection and deflection measured at distance  $x$  from load center, respectively. And finally, decrease in HMA modulus was also modeled as function of initial modulus as:  $E_n/E_{ini}=1-0.5*n/N$ , where,  $E_n$  and  $E_{ini}$  are moduli of HMA at  $n$  number of load application and initial modulus respectively,  $n$  and  $N$  are current number of load application and number of load application for which modulus of HMA reduces by 50 percent of initial value respectively. It was concluded that these performance models could be used in predicting pavement life in actual in situ pavement.

White *et al* [7] presented the analysis and discussion of the test results obtained from the APT using Indiana Department of Transportation/Purdue University prototype scale APT facility. The objective of the study was to evaluate the effect of many factors such as pavement geometry, boundary conditions on the rutting behavior of the pavement. The overall goal was to have an early evaluation of superpave rutting resistance. The scope of the study included the following:

1. Test sections were prepared with a high and a low-density section. Each paving lane was 3 meter wide.
2. Samples were collected to determine the asphalt content and gradation.
3. Tests were run at 50°C temperature and profiles were measured at regular intervals of 0.6 m by profilometers.
4. Traffic was applied with single wheel path as well as with wander.
5. Profiles were recorded at nine locations, however three consecutive sections nearest to the center of the test section were averaged and used as a single result.
6. Slabs cut from APT test sections and laboratory blended, mixed and compacted sections were tested with Purdue University Laboratory Wheel Track tester (PURWheel) to examine any difference in performance of field and laboratory compacted slabs.
7. A finite element analysis was performed to calibrate the creep rate model using the actual data of APT. A reasonable agreement was achieved between the measured and predicted rutting.

The above study showed that the finite element method could be used to model the rutting and the rutting in slabs compacted in laboratory was different for slabs compacted in field.

Harvey *et al* [8] discussed the results obtained from the heavy vehicle simulator test done as per the CALTRAN'S APT program, which was a joint effort by CALTRANS and the University of California, Berkeley (UCB). One of the HVS test was done at UCB in a controlled environment and the other was done at in-service pavement. The objective of the study was to discuss the results of the CALTRAN's APT program obtained since 1994 to 1998. The scope of the study included the following:

1. There were two types of pavement structure used for the test with asphalt concrete, aggregate base (and asphalt treated permeable base), aggregate subbase and subgrade.
2. The design and analysis system for fatigue has been discussed. Mix response fatigue characteristic was represented by the equation:  $N = a(1/\epsilon_t)^b$ , where  $N$  = no of load application to failure under the tensile strain  $\epsilon_t$  and  $a$ ,  $b$  = mix specific coefficients determined by the test. The number of Equivalent Single Axle Load (ESAL) that could be sustained in the HVS program was determined by the relation  $ESAL = N*SF/(TCF*M)$ , where  $SF$  = shift factor to adjust the difference between the fatigue in laboratory and at in-situ,  $TCF$  = Temperature Conversion Factor,  $M$  = reliability multiplier.
3. Investigation completed through June 1997 had been presented with the results of tests on fatigue performance of asphalt concrete mixes and influence of several parameters such as mix proportions and air void contents on the fatigue life of asphalt concrete.
4. Results of accelerated HVS tests on four full-scale pavements were presented. They showed the fatigue performance of test sections.
5. The other results presented of the HVS study on full-scale pavements included the study on asphalt treated permeable base and permanent deformation study of mix.

Based on the review of the results obtained in HVS study, following conclusions were drawn:

1. The designed thickness of HMA was found to be adequate in terms of permanent deformation performance, while the same was found to be inadequate in terms of fatigue performance.

2. It was found that the use of asphalt treated permeable base under the dense graded asphalt concrete should be reconsidered because of the reduction of permeability of asphalt treated base. It was concluded that by reducing the permeability and cracking potential of asphalt concrete, the necessity of asphalt treated permeable base could be eliminated.
3. Proper construction practice was found to be necessary to increase the fatigue performance of asphalt concrete.

### **4.3 Other Accelerated Testing Using HMA Samples**

There are several types of accelerated loading equipment available for testing laboratory compacted samples, such as, the Asphalt Pavement Analyzer (APA), originally known as Georgia Wheel Tracking Device [9], which is used for testing performance of laboratory compacted samples of Hot Mix Asphalt (HMA) under controlled environmental condition. Both gyratory compacted cylindrical and vibratory compacted beam specimens can be used. In the APA, a rubber tube filled with air pressure between 518 kPa to 690 kPa is placed on top of the sample and repeatedly rolled over by wheels with loads from 34 kg to 45.5 kg for many cycles to produce rutting failure. The sample is either kept immersed in water or put into an environmental chamber under a controlled temperature (between 35°C and 40°C). Fatigue performance of HMA can be predicted by repeated load Indirect Tensile Test (ITT) using a Universal Testing Machine (UTM) [10] and also with the four point bending fatigue test apparatus; both being equipped with environmental chamber. Apart from these common devices, there are a few wheel tracking devices, which are primarily used for evaluation of stripping and rutting potential of HMA in the laboratory. Examples are: (i) Hamburg wheel tracking device [11], which uses a sample size of 26 cm × 32 cm × 4 cm and temperature of 50°C and loads of 705 N. It has a steel wheel of 4.7 cm diameter, which passes 50 times over each sample every minute. (ii) French rut tester [12] which applies 5 kN load with 600 kPa tire pressure at 40°C to 60°C and uses samples in a mold of dimension 50 cm × 18 cm × 10 cm. Pavement test slabs are compacted using a Linear Kneading Compactor.

The wheel tracking devices mentioned above have been primarily used for rut tests. Four point bending test is the most widely used laboratory test method for assessing fatigue potential of HMA. From the point of view of accelerated tests in the laboratory, the aforementioned devices are not considered appropriate candidates as accelerated loading tests because of the nature of their loading. Furthermore, from the point of view of model tests in the laboratory, it is important to note that to simulate conditions comparable to field conditions, laboratory samples should be prepared in a way, which is similar to the method of field compaction. Moreover, the theory of model testing requires “similarity” between the ‘experimental model and test conditions’ and the ‘prototype and test conditions’ must be achieved so that the experimental results are comparable with prototype results. In other words, all dimensionless properties should have the same value for both the model and the prototype. The immediate consequence of this in pavement testing is that “geometric similarity” should be achieved in any testing, that is, all linear dimension of the model should be related to corresponding linear dimension of the prototype by a scale factor. Therefore, for the purpose of evaluating response and performance of pavements a device is needed that is able to test a composite pavement while maintaining the similarity principle. This rules out devices that test either circular cylinder or beam samples. Since none of these tests can be performed with the presence of base and/or subgrade material, it does not maintain a similarity principle and therefore, the samples tested under these ‘accelerated’ testing environment are not comparable with the field conditions.

#### **4.4 Small-Scale APT**

Tests conducted in full-scale facilities are time consuming and expensive due to large number of influence factors that have to be taken into account. As reported by Van-de-Ven *et al* [13], there may be a need to perform preliminary testing prior to full-scale testing to monitor the effect of change of different variables. This requires a testing facility with lower cost, which can control specific variables directly. To conduct “true” accelerated testing on a representative pavement structure in the laboratory, one needs a facility to prepare a test bed with the same material profile in vertical direction as in the

field with a reduced scale, and a loading device that is itself calibrated and designed to maintain similarity. Moreover, a quick test on performance of mix on a test bed may require a laboratory facility, which can be set up at short notice and moved easily inside the laboratory.

This can be done by an accelerated testing facility, which uses scaled down load and pavement geometry in laboratory. In this type of loading, a scaling factor is applied between the full-scale prototype pavement and the scaled model. A dimensional analysis is performed to determine various scaling factors necessary to apply to different parameters, such as, geometry, loading and material so that the same strains and stresses are obtained in the model as in prototype. The details of the dimensional analysis can be found in [13], [14] and [15].

Let  $N$  be the scale factor applied between prototype and scaled pavement structure. If dimensions are scaled down by the factor  $N$ , forces should be scaled down by a factor  $N^2$  to have same stress in scaled pavement as in prototype. Moreover, since we are interested in the same performance of scaled pavement over time as the prototype pavement and HMA is a viscoelastic material, whose response changes with time, the time length should be same for scaled and prototype pavement. Therefore, if 1: $N$  be the ratio between scaled and prototype pavement dimensions, the velocity should be scaled as 1: $N$  because velocity = length/time. These results are based on the fact that inertial effects are negligible in scaled and prototype pavement; only viscoelastic effects are present. Kim *et al* [15] reported the findings of analytical studies performed to find the factors governing inertial effect. It was reported in that study that with velocity less than 62 mph, the inertial effects are negligible. Therefore, for scaled pavement structure, following scaling factors should be employed in order to have the same response in scaled pavement as in prototype:

Dimension (thickness of HMA): 1: $N$

Material Properties: 1:1

Load: 1: $N^2$

Stress: 1:1

Velocity: 1: $N$

An important study on fatigue performance of HMA using a small wheel tracking device in the laboratory was performed by Van Dijk [16]. In this study, rectangular HMA slabs of dimension 950 mm X 440 mm X 40 mm were tested under moving wheel load. The slab specimens were compacted under hand driven roller in a mold and then sawed into rectangular shapes. They were later transferred to rubber foundation of thickness 80 mm. Strain gauges were glued under the slabs along longitudinal and transverse directions. The slabs were tested under 0.016 kN bi-directional wheel at 20°C. Top and bottom of wheel path were photographed in regular interval to monitor the development of cracks. Transverse and longitudinal strain gauges showed different magnitude of strains. Since a range of strain values and corresponding failure loads were required to draw  $N_f$ -vs-strain curve and wide range of strain values were obtained from transverse and longitudinal strain gauges from a single slab, it was commented that data from a single slab could be used for drawing  $N_f$ -vs-strain curve. Strain histories for all strain gauges indicated following distinct points: (a) initially there is almost no change in strain values, (b) followed by a point at which strain started to increase (at load  $N_1$ ), (c) then reached a point of maximum strain (at load  $N_2$ ) and (d) followed by a decrease in strain until failure (at load  $N_3$ ).  $N_1$  and  $N_2$  were correlated with initial strain. This gave two equations:  $N_1$ -vs-strain and  $N_2$ -vs-strain. By correlating the crack development with the strain gauge values it was concluded that, (a) before  $N_1$ , hairline cracks are initiated; (b) between  $N_1$  and  $N_2$ , hairline cracks widen to form network, (c) after  $N_2$ , real cracks are formed followed by (d) a failure at  $N_3$ . This gave the understanding of fatigue characterization of the mixes in terms of crack initiation and real crack development. The results indicate that  $N_2$ -vs-strain curve gives failure load values in the order of 3 times greater than that obtained from  $N_1$ -vs-strain curve. The lower value of slope obtained through wheel tracking test was noted in the discussion part of the study. It was also noted that, since  $N_2$  values corresponds to situation of real crack development and controlled strain tests also correspond to same situation (in contrast to controlled stress tests where failure is primarily dependent on initial crack development), controlled strain data should be used for design of pavement.

Several important points are apparent from the study results:

1. Since the loading was bi-directional, the strain signals obtained from ends of the slab were of duration two times greater than those obtained from middle of the slab. The strain gauges between the ends and the middle of slab showed two peaks very near to each other followed by a longer rest period than the other strain gauges due to the fact that two wheel loads acted in different directions in quick succession and these strain gauges were not counted for analysis. The overall involvement of different strain gauges caused mixing up of signals of different frequency, which should be avoided in fatigue characterization.
2. Strain gauges in different directions were used to develop fatigue equations. But, a question still remains whether this is theoretically possible or not because of qualitative difference in response of HMA in two mutually perpendicular directions under wheel load.
3. It has been reported in the study that while the scale between slab thickness in the laboratory and field thickness was about 3.5 to 5, the loading scale between laboratory and field was about 13 to 25, which satisfied the scaling criteria discussed earlier in this section.

Another important study on validation of fatigue performance of HMA using a small wheel tracking device in the laboratory has been performed by Rowe and Brown [16]. The objective of the study was to evaluate fatigue performance of different mixes in the laboratory. The wheel tracking device consisted of a bi-directional wheel, which could create pressure of maximum 650 kPa. The study used 380 kPa pressure with loads varying from 0.6 kN to 5.4 kN. The test bed consisted of rectangular HMA slabs of dimensions 1000 mm x 500 mm x 50 mm. A hand driven single drum pneumatic roller was used to compact the slab to the desired thickness. The test slabs were fixed with strain gauges in both longitudinal and transverse direction under the slab. The test slabs were mounted on top of a rubber mat to provide a flexible support and the wheel loads were applied on top of the slab. The strain gauge outputs were recorded and important characteristics such as permanent strain and transient strains were monitored. Two important points to be noted are: (i) the direction of the wheel load was bi-directional instead of unidirectional as in the case of a particular lane of an actual pavement and (ii) no particular scale over prototype pavement structure was used for developing the model.

These two studies show the necessity of using wheel tracking device using proper scale between model and prototype pavement using unidirectional loading. A laboratory equipment which meets the criteria of a scaled model is the Model Mobile Load Simulator (MMLS). In early nineteen nineties, the one tenth scale Model Mobile Load Simulator was used in laboratory tests for evaluating mix performance under variation of different material parameters [13]. Subsequently, the MMLS3, a nominally one third scale trafficking device was developed and since 1997 it has been extensively used by several researchers for accelerated trafficking of field pavements to evaluate response and performance in terms of rutting and fatigue. Since the MMLS3 equipment consists of a test bed and a loading device, which can be relocated in the laboratory easily, it has the potential of becoming one of the prime tools for accelerated testing for mix performance. A brief history of MMLS3 is provided in the next section with reference to specific published literature and the potential of the use of MMLS as a tool for testing pavement materials is identified.

#### **4.5 Brief History of MMLS3**

A 1:10 scale model of MMLS has been used in a controlled environment to perform scaled pavement studies for rutting and fatigue [13]. Van-de-Ven *et al* [13] presented a summary of results obtained from rutting tests performed with this device in University of Stellenbosch, South Africa and fatigue tests performed at University of Texas at Austin, Texas (the necessary references can be found in [13]). The 1:10 scale model of MMLS consists of a mold for preparing a scaled model of a pavement and the loading equipment. The mold has the size of 3000 mm x 1100 mm x 20 mm. The loading device uses a wheel load of 200 N with double bogie and solid 25 mm wide tire. It has a maximum velocity of 1.1 m/s and could provide 10,000 passes per hour. The scaling of the pavement was done in order to attain similitude (as explained before). For this study, the gradation of HMA was scaled down to 1:10 upto material passing 0.075 mm sieve. This made the filler fraction almost doubled in scaled pavement compared to the field and hence increased the aggregate surface area significantly. Therefore, a high binder content was necessary to produce desirable volumetric properties. To maintain same void

content, volume of the aggregate had to be reduced also. The stiffness of the mix thus obtained was 2087 MPa for scaled model compared to 3258 MPa for full-scale model (both Marshall compacted). Permanent deformation tests were performed to investigate the effect of variation of binder content with and without laboratory aging effect. Fatigue tests were carried out at 5°C temperature with a scaled model, where half of the trafficked area was aged artificially. The continuous deterioration of pavement stiffness was monitored with Spectral Analysis of Surface Wave (SASW) and cumulative surface cracking were measured during trafficking. It was concluded that the MMLS 1:10 model could be successfully utilized to investigate the mix response under various loading parameters provided proper scaling was performed. The difference in mix stiffness between full scale and scale down model also has to be taken into account when comparing the results between them, because they affect the mix performance in fatigue and rutting.

One of the difficulties of the 1:10 scale model was that scaling down of gradation eventually increased the filler content of the mix and that had an effect on the mix performance. The difference in volumetric properties due to scaling had an influence on the fatigue life, which was measured using MMLS 1:10 [13]. A new model of the device, which uses 1:3 scale of full scale pavement geometry and loading was then developed and is being used successfully in field to monitor rutting and fatigue potential of the mix. This device, known as MMLS3, consists of a bigger mold and a bigger loading equipment. This device can be either used in field by placing directly on the pavement or can be used in the laboratory on a model scaled layered pavement structure of size 2744 mm x 915 mm x 305 mm. The total 305 mm depth can be used to compact different layers of the pavement, which are being simulated. All the layers are scaled down and compacted using a hand driven steel vibratory roller. The layers are prepared one after another from the bottom once adequate density is achieved in each layer. The loading equipment has 4 bogies, 1 axle per bogie and 1 wheel per axle. It has four tires each 80 mm wide, with maximum inflatable pressure of 800 kPa, and between 1.9 kN to 2.7 kN axle load. The nominal wheel load application rate is 7200 per hour with 2.5 m/s nominal speed. The dimensions of the device are 2400 mm x 600 mm x 1150 mm and it weighs 800 kg. An environmental chamber can be placed on the mold and temperature of the test

pavement can be controlled through air blowers from both sides. Load can be controlled by adjusting the spring in the axle system and the tire pressure can be controlled by inflating and deflating the tire. Since a single wheel load in the field is 40 kN to 50 kN, a scaled down load of 2.7 kN means applying a scaling factor of 3.8 to 4.3 ( $1:N^2$  for load). The load is adjusted accordingly for any other scaling factor, such as 3. It has been mentioned in [13] that it is more practical to use MMLS3 to test scaled down model of pavement structure. However, there is not any published literature (to the knowledge of the author of this document) available today on the use of MMLS3 in laboratory on material characterization of laboratory compacted mixes. There has been some study performed on the use of MMLS3 on verification of performance of HVS and comparison of rutting and fatigue results from MMLS3 and HVS at field. They are summarized bellow.

Hugo [18] studied the fatigue and rutting performance of full-scaled pavement on the northbound inside lane of US281 near Jacksboro, Texas. Cores were extracted from the pavement after trafficking and fatigue test was performed in the laboratory at 10 Hz and 20°C with no rest period. The results showed that the asphalt initially gained fatigue life due to the compaction of asphalt layer by wheel loads, and the fatigue properties deteriorated under further traffic. The same trend was observed with the SASW stiffness measurement. The average maximum rut deformation in the top 90 mm under load was also observed. The ratios of the areas under stress distribution curves for full scale TxMLS and MMLS3 loading conditions could be used as an indicator of prediction of rut depth, which was shown to be true for this study.

The results obtained from TxMLS and MMLS3 on US281 near Jacksboro, Texas has been compared and reported by Hugo *et al* [19]. This paper discussed the APT done at Jacksboro, Texas, using the MMLS3. The test was done to compare the results obtained from the full-scale TxMLS study performed earlier at the same place. Both wet and dry tests were performed; in the wet tests water was flowed over the test surface to induce moisture damage.

The objectives of the study were:

1. To perform a wet test to observe the stripping phenomenon under the action of water.

2. To perform a dry test to compare the performance between MMLS3 and TxMLS.
3. To perform laboratory test to determine material characterization.

The scope of the study included the following:

1. The one-third scaled model of MMLS3 was used a selected portion of the pavement. A grid was laid on the pavement surface and the profilometer was mounted on.
2. A water system was mounted with the MMLS3 for the wet testing, which simulated 1 mm thick water layer equivalent to 5 mm/hour rainfall intensity.
3. Cores were obtained in and between the wheel paths for determination of VTM, VMA, moisture susceptibility, repeated shear test and frequency sweep test.
4. As per the data collection program, profilometer data was obtained and SASW data was obtained from fourteen locations. Temperature was also monitored during the test.
5. From the data obtained, rutting was determined for the dry part of the test and was compared with the rutting of the full-scale pavement under TxMLS.
6. SASW values were compared with the same values from TxMLS test.
7. Cracking was observed for the wet part of the test.
8. A discussion was presented next where the details of the model testing was presented with particular reference of using MMLS3 in field. Then, the discussion on a stress/strain analysis, performed with ELSYM5 to compare the vertical stress response under TxMLS and MMLS3, was presented. Performance of pavement structure under the full-scaled and model loads regarding the permanent deformation and loss of stiffness was presented. Finally, a discussion on the results of laboratory testing on the volumetric properties, moisture sensitivity, shear testing and frequency sweep test was presented.

Based on the above MMLS3 study, the following conclusions were drawn:

1. MMLS3 was able to predict the performance of pavement in terms of fatigue and permanent deformation.

2. From the laboratory tests, it was found that the upper layer of the pavement structure was more susceptible to stripping and less prone to rutting due to high shear strength. MMLS3 results correlated with these findings.

In another study by Hugo and Poolman [20], the rut data obtained from the MMLS3 study of one-third scale model by TxDOT at Westrack pavements under two different loading conditions were critically analyzed. This report presented an analytical study on the data recorded from an earlier MMLS3 study by TxDOT at West track pavements under two systems of load. Several corrections on the measured profilometer reading had been discussed in the report.

The scope of the study included the following:

1. Consideration of possible errors in measurements:
  - a. The error in initial set up of the profilometer resulted many profiles to be not aligned horizontally. The non-overlapping rut profiles were shifted horizontally to compensate this effect of measurements.
  - b. The effect of different drop height of profilometer wheel as well as non-horizontal set up of the profilometer resulted the profiles in many situations to be shifted vertically. They were then adjusted vertically and rotated with respect to each other to compensate the difference in setup of the profilometer.
  - c. The profiles were also adjusted to compensate the effect of flexural rigidity of profilometer beam.
  - d. A regression model was developed which was used to minimize the sum of the squares of the errors in profilometer readings in the un-trafficked regions between profiles at the beginning and after trafficking. The rut depth was calculated as the maximum difference between the profiles before and after the trafficking after performing all of the above corrections.
2. Consideration of lateral flow of asphalt:
  - a. To compare rutting under the truck traffic and MMLS3 loading, a comparable load application method was proposed which could take care of the lateral movement of asphalt during trafficking.

- b. Secondary effect like the upheaval of asphalt due to the trafficking outside the designated comparison zone was mentioned to be important to be considered for comparison between two types of traffic.
- c. The variation of rutting over the variation of applications of MMLS3 loads had been plotted for various sections of the pavements where the tests were run. The best-fit curve was obtained considering the shoving of the asphalt material during the test.

A final summary of the results was presented where the sections were ranked based on performance on rutting.

Hugo and Poolman [21] and Epps *et al* [22] presented the determination of several factors, which could affect the results of MMLS3 testing by TxDOT in Wes Track.

The objectives of the study were the followings:

1. To identify several factors, which could influence the main hypothesis that the extent of rutting is dependent on the vertical stress distribution under the tire, the material characteristics and structural composition and prevailing conditions during trafficking.
2. To formulate an analytical procedure to quantify the rutting behavior of pavements.

The scope of the study included the following:

1. The procedure followed to analyze the rut data included the following steps.
  - a. Elastic stress analysis under the two system of loading (the truck loading and MMLS3 loading) of the pavement structure was done using the ELSYM5. Different values of elastic stiffness of layers were used with the same value of Poisson's ratio of 0.35.
  - b. For each layer the Stress Potential (SP) was determined.
  - c. A visco-plastic analysis was also performed to determine a Temperature Frequency Correction (TFC) value.
  - d. Combination of elastic and visco-plastic analysis resulted in the determination of Rutting Potential Ratio (RPR).

- e. Comparative Load Rut Ratios (CompLRR) was determined for the pavement structure to account for the differences in lateral wander between the tests.
  - f. Theoretical Rut Ratio (TRR) was calculated as the product of RPR and CompLRR.
  - g. Field Rut Ratio (FRR) was calculated from the profileometer data.
  - h. The analysis ended with the determination of Prediction Ratio for Rutting (PRR) for each section of the pavement from the values of TRR and FRR.
2. The effect of material characterization and structural composition on the analysis of rut data has been studied in the following steps:
- a. Deformation within the pavement layers: It was observed that the permanent deformation occurred inside the pavement surface throughout the HMA layer instead of the previously assumed top 75 mm of HMA layer.
  - b. Stiffness of asphalt layer: The  $G^*$  value of HMA was determined at the time of placing of layer prior to trafficking and after trafficking. The value of  $G^*$  increased after trafficking due to densification under traffic load. It had the positive effect on the stiffness of the asphalt layer. On the other hand, the effect of aging had a negative effect on stiffness. It has also been mentioned that acute increase of stiffness occurs within 15-20 mm layer after several years due to ultra violet radiation.
  - c. The Young's modulus  $E$  was determined by the four point bending test and was used in the initial phase of the analysis. Later in the modified analysis procedure explained above,  $E$  was calculated from  $G^*$  using the relation  $E = 2G^*(1+k)$ , where  $k$  is the Poisson's ratio.  $E$  values of the upper layers were calculated based on the values of lower layers by method of proportions and also on the basis of indirect tensile test values.
3. Several factors influencing the stress analysis were also mentioned as:
- a. Effect of temperature of tire pressure can in turn affect the stress distribution under the tire.

- b. Loading characteristics: Because of the wandering effect of pavement, path of loading changed the loading pattern on the pavement.
- c. Stress profile along the depth was analyzed to determine what the effect would be if the deformation occurs throughout the asphalt layer (not at top 75 mm layer), which was observed in reality.

Based on the above study it was concluded that the hypothesis mentioned at the beginning of this review held good for the all the test sections provided all the factors affecting the points of hypothesis were considered properly.

In a following study by Epps *et al* [23], the performance prediction methodology of MMLS3 to predict rutting in actual pavements has been presented in detail. Primarily the objective of the study was to validate the hypothesis of comparable stress distribution under MMLS3 and under full scale loading and compare the theoretical and measured rutting to validate performance prediction methodology. The comparable stress distribution means that for a pavement structure with single HMA layer, the stress at a depth inside HMA layer under full scale loading under one wheel of single axle will be same as stress at one-third depth under MMLS3 loading with same tire pressure as full scale. According to this hypothesis and equivalent environmental and material condition, the rutting under full scale loading will be three times the rutting under MMLS3. The performance prediction methodology required that Theoretical Rut Ratios (TRR) be equal to Field Rut Ratios (FRR), where rut ratio means the ratio of rutting between MMLS3 and full scale. With the hypothesis that rutting is proportional to area under maximum vertical compressive stress curve within a layer, which was defined as Rutting Potential (RP), Rutting Potential Ratio (RPR) was defined as ratio of RPs of MMLS3 to full scale. When the MMLS3 test temperatures are different than the field test temperatures, Temperature Correction Factors (TCF) were applied to RPR to obtain the TRR as equal to the product of RPR and TCF. When TRR is equal to FRR, the Rut Depth (RD) under full scale becomes equal to the ratio between RD under MMLS3 and TRR. The results of accelerated testing of actual pavement structure in Jacksboro, Texas was used to validate the hypothesis of comparable stress distribution and equality of TRR and FRR. ELSYM5 software was used to validate the comparable stress distribution under two hypothetical pavement structures and it was shown that the hypothesis held good, thus validating the

1/3 factor between full scale RD and MMLS3 RD. For hypothetical structure, the RD of full scale was three times the RD of MMLS3 when a scaled portion of full HMA layer was used. For actual pavement structures tested, TRR and FRR were approximately equal when TCF and loading differences were accounted for. Thus, MMLS3 was validated as a tool for performance prediction in terms of rutting under full scale loading condition.

MMLS3 has even been used as a tool for evaluating performance of HMA under wet condition as reported by Smit *et al* [24] and Walubita *et al* [25]. Tests under wet conditions were conducted in varying temperature conditions and it was observed that MMLS3 was able to simulate the effect of water damage (stripping) and associated stiffness loss in HMA.

The only literature (available to the author of this document till today) on use of scaled pavement testing using MMLS3 in the laboratory is the one by Lee and Kim [26]. The study reported by Lee and Kim [26] was a step forward in the direction of establishing a fatigue test protocol of HMA using scaled pavement structure in the laboratory. In this study, the main objective was to investigate that whether MMLS3 can be used to simulate fatigue failure in scaled pavement in terms of alligator cracking, strain increase and reduction of stiffness. The rutting due to loading was measured using profilometer and also using dial gauges. The cracking in pavement was monitored by drawing the crack patterns in Plexiglas and also taking digital photographs. The continuous deterioration of stiffness of HMA was observed by using PCB A402 accelerometers and analyzing surface waves. The strains under the pavement were observed using strain gauges of length 50 mm at the bottom of test slabs in direction transverse to wheel load direction. Several scaled pavements were tested. The first slab tested was a 40 mm thick HMA slab on 160 mm gravel base followed by sand subgrade. It was observed that high stiffness of gravel base did not cause fatigue failure even after 2.5 million loads. In next trial, base was removed and 80 mm thick slab was rested directly on subgrade and it was observed that fatigue failure did not occur even after six (6) million load applications in six (6) months due to increased thickness of HMA. Therefore, in third trial, 60 mm thick HMA slab was placed on top of six 25 mm thick D60 neoprene sheets, which were rested on a 20 mm thick steel plate followed by sand subgrade. Neoprene layer was selected because its modulus was similar to that of the

base and it facilitated the effort of putting strain gauges under HMA slab. The test slab was fixed with neoprene layer using a tack coat. Longitudinal hairline cracks were observed after 1.5 million load applications but no visible alligator cracking was observed. In the next part a similar but 40 mm thick HMA slab was tested. The result was that both longitudinal and alligator cracking was observed. Strain time history under the test slab showed a quick increase at the initial loading stage (primary stage); then increased almost linearly (secondary stage) followed by an exponential increase in the tertiary stage. The failure strain was determined by the intersection of straight lines between secondary and tertiary phase, and the corresponding load was chosen as failure load. The phase velocities measured from surface wave analysis showed the reduction of stiffness during loading. The reduction of stiffness by 50% in the presence of cracks was chosen for failure criteria. A cumulative damage analysis was carried out to determine the damage ratio. To determine the failure load as function of strain and modulus of HMA, the Asphalt Institute method based on phenomenological evidence was used. The strain was the initial amplitude of strain observed at stabilized variation of strain and the modulus was back calculated using elastic layer theory to match the calculated strain at the bottom of the HMA with the observed strain. The failure load thus predicted was 0.143 million compared to 0.145 million observed in the test. At the end, it was concluded that a test protocol could be set up using MMLS3 to observe fatigue related damage in HMA as well as a tool for material characterization of HMA.

#### **4.6 Conclusions from Literature Review**

After going through the above review of literature, it can be realized that there had been a wide range of situations where the accelerated pavement testing has been performed. However, it can be concluded that in almost all of the above tests the main emphasis was to get reliable data on APT so that better design alternatives could be achieved.

*Importance of scaled model:* It can be concluded from the review that while full-scale testing facilities provide field results directly, small scaled testing facilities provide better

control of test variables within reasonable cost and time. Several small scaled test studies have been reviewed and following general conclusions can be drawn from them:

1. Small scaled APT facilities can be used for material characterization of HMA in the laboratory.
2. When a proper dimensional scaling factor is employed over the prototype structure and loading, the response of the resulting model pavement should be directly comparable with a prototype pavement structure.
3. Most of the studies on scaled pavements have examined the permanent deformation behavior of HMA. While rutting is one of the important factors of design, fatigue is an equally important factor. While there are several studies performed on fatigue characterization of HMA in the field using scaled model, the reported studies on fatigue characterization of HMA in the laboratory are few. Those reported studies in the laboratory do not simulate the loading pattern encountered in the field and no general test protocol for using scaled models simulating field conditions closely in the laboratory has been developed.

The study reported in this dissertation attempts to establish a test protocol for using MMLS3 scaled pavement models for fatigue characterization of HMA in the laboratory.

## Chapter 5

### NEED FOR THE PRESENT STUDY

#### 5.1 Need for Detailed Test Protocol

A review of literature reveals that there is only one use of scaled model pavement in the laboratory for fatigue characterization [26] and there was no detailed test protocol presented in that study. Results from two tests cannot be compared without a proper protocol, therefore, there is a need for establishing a detailed test protocol for using MMLS3 for testing scaled models of pavements in the laboratory. This has been discussed in the chapter “Development of Model Pavement and Test Protocol Using MMLS3”.

#### 5.2 Need to Represent Field Conditions Closely in Laboratory

As discussed before, a wide variety of accelerated loading facilities in the laboratory are available to determine and verify performance of a particular HMA material in pavement. However, a close look at these tests reveals that although they do perform accelerated loading, they fall short of simulating exact field conditions. This is because existing facilities do not consider the effect of underlying layers. This is explained in detail in this section by comparing performance of indirect tensile tests and four point bending test, both of which are widely used in determining fatigue properties of HMA.

##### 5.2.1 Indirect Tensile Test

To begin with, we consider the strain distribution in an indirect tensile test. Following the theory of elasticity of deformable bodies [26], the elastic strain along horizontal diameter due to load  $P(t)$  along vertical diameter of the disk is given by:

$$\varepsilon(x,t) = \frac{1}{\pi L d E} \left[ -2(1-\nu) - \frac{8d^2}{(d^2 + 4x^2)} (4x^2 - \nu d^2) \right] P(t) \quad (5.1)$$

where,  $x$  and  $t$  denote distance along diameter and time,  $L$  and  $d$  are the length (thickness) and diameter of cylinder,  $\nu$  is the Poisson's ratio and  $E$  is the elastic modulus of HMA. Upon substitution of  $x=0$ , the maximum strain at the center of the disk is given by:

$$\varepsilon(t) = \frac{2(1+3\nu)}{\pi L d E} P(t) \quad (5.2)$$

When **Eq. 5.1** is integrated over a finite length  $c$  along the diameter, the total deformation is obtained as:

$$\Delta_c(t) = \int_{-c/2}^{c/2} \varepsilon(x,t) dx \quad (5.3)$$

The elastic modulus is obtained by integrating over whole diameter as:

$$E = \frac{\nu + 0.27}{L \Delta_d(t)} P(t) \quad (5.4)$$

**Equation 5.4** is used for the calculation of the resilient modulus of HMA with  $P(t)$  replaced by the peak load application.

### 5.2.2 Four Point Bending Test

Next, we consider a four point bending test where we apply a constant bending moment between two point loads. From either a stress controlled or strain control test, the fatigue characterization curve for the sample is developed. For stress-controlled tests, strain increases due to viscoelastic nature of the material and for strain-controlled tests, the stiffness of the sample decreases as test progresses. In either case, the strain at the bottom fiber of the beam is calculated in every cycle of load application, which is given by:

$$\varepsilon_x(t) = \frac{2L}{bh^2 E} P(t) \quad (5.5)$$

where,  $b$  and  $h$  are the height and depth of the beam and  $L$  is the length between two outer supports of the beam.

Comparing Eq. 5.1, 5.2, and Eq. 5.5 it can be seen that, the elastic strain at a particular point can always be written in form:  $\varepsilon(t) = A \frac{P(t)}{E}$ , where  $A$  is independent of  $E$ , but a function of the location where the strain is being calculated, geometry and boundary conditions of sample under test and Poisson's ratio. This proves that elastic strain is directly proportional to load and inversely proportional to elastic modulus for the tests considered here. Although there can be various ways to express elastic strain, this form of the equation is also useful when dealing with linear viscoelastic assumption of HMA because it can be directly converted to a linear viscoelastic solution using the correspondence principle and Boltzman superposition integral. The linear viscoelastic solution thus becomes:

$$\varepsilon(t) = A \int_0^t J(t-u) \dot{P}(u) du \quad (5.6)$$

where,  $J(t)$  is creep compliance of HMA under tension.

Therefore, by suitably altering these properties we can use either indirect tensile mode or four point bending mode to achieve desired strain and stress level. However, this equation is not directly applicable to actual field conditions where presence of underlying layer makes the situation different. This can be explained if we consider a typical four-layered pavement. The parameter  $A$  is shown against several values of modulus of HMA in Figure 5.1.

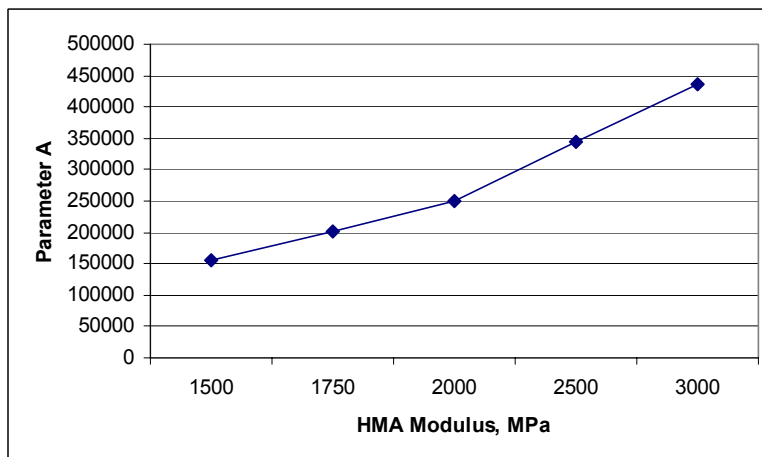


Figure 5.1: Effect of HMA elastic modulus on the parameter 'A'

As **Figure 5.1** indicates,  $A$  is a function of the HMA modulus  $E$ . In a similar way, it can be shown that  $A$  is also function of the modulus of the underlying layers as well as some other parameters, such as layer thickness, Poisson's ratio. Therefore, the above equation is modified to  $\varepsilon(t) = A(E_i, i = 1, 2, \dots) \frac{P(t)}{E_1}$ , where,  $E_i$  are modulus of  $i$ th layer with  $E_1$  being modulus of HMA. Therefore, the problem is clearly nonlinear in nature and linear time dependent viscoelastic solution cannot be obtained through Boltzman superposition principle. Therefore, the linear viscoelastic behavior of HMA can only be simulated in conventional tests. The exact form of  $A$  is a function of all layer moduli.

Another important difference between conventional tests and actual field or MMLS3 tests is that conventional tests consider one-dimensional behavior while full scale and/or MMLS3 simulates three-dimensional behavior. This is explained here by comparing results obtained by three-dimensional finite element simulation of MMLS3 and full-scale model.

### **5.3 Need to Develop Fatigue Characteristic Curves of HMA in the Laboratory Using Scaled Model**

The primary objective of any fatigue related study is to obtain the characteristic curve ( $\log(N_f) - \text{vs} - \log(t)$ ) for the mix being tested. The study in reference [25] reported one data point along the curve because results of one the test slab were presented. On the other hand, development of the characteristic curve requires results of many tests carried at different strain levels; therefore, tests of several slabs are needed. This will be discussed in **Chapter 10**.

### **5.4 Need to Investigate Effect of Factors on Fatigue Performance**

Since permanent deformation or rutting is caused by the shear failure from both sides of the wheel path, it is expected that it can affect the fatigue behavior. The review of the literature reveals that conventional fatigue test methods (e.g. beam fatigue, indirect

tensile test fatigue) consider permanent deformation behavior and fatigue behavior separately, while in real field conditions they occur simultaneously. Therefore, it is essential to simulate field conditions in laboratory where these two effects can be observed simultaneously and the effect of rutting on fatigue can be investigated. This is discussed in the chapter “Test Results and Analysis”.

### **5.5 Need to Develop A Model of Test Pavement To Estimate Time Dependent Strain**

HMA behaves elastically during the initial stages of repeated loading and viscoelastically during later stages when strains increase with time until failure. These elastic and time dependent behaviors should be modeled in a suitable way to estimate strains at any point of time. This is discussed in **Chapter 10**.

## Chapter 6

# EQUIPMENT AND MATERIALS

### 6.1 Introduction

In this chapter, the MMLS3 and the pavement materials used for this study are discussed. A brief description of the MMLS3 with specifications is followed by the descriptions of the materials.

### 6.2 Model Mobile Load Simulator Mk3 (MMLS3)

The MMLS3 consists of the following parts:

- (1) The loading equipment,
- (2) The compaction equipment and mold and
- (3) The environment chamber.

#### (1) The Loading Equipment

**Figure 6.1** shows the longitudinal cross section of main loading equipment of MMLS3.

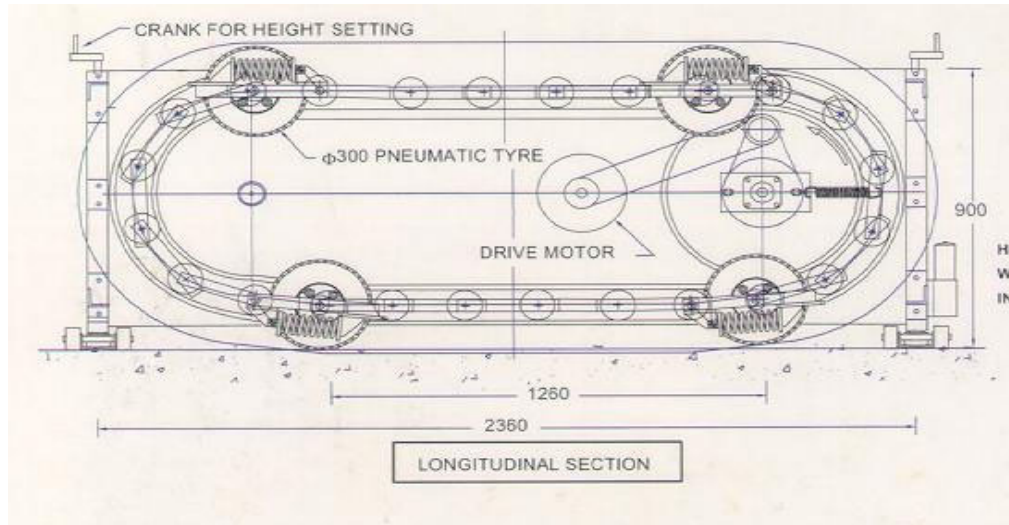


Figure 6.1: A longitudinal cross section of loading equipment of MMLS3

As indicated in **Figure 6.1**, the loading equipment consists of four wheels spaced at 1260 mm. A motor drives the wheels using a belt drive system. The four main wheels are connected by a flexible steel chain, which rotates around a steel rim over several small steel wheels. Each of the four main wheels consists of a 300 mm diameter pneumatic tire. The load on each of the four wheels is controlled by adjusting the tension in the spring attached between the wheel and chain which is further controlled by adjusting the height of the equipment. The height of the equipment is adjusted by four crank handles.

## (2) The Compaction Equipment and Mold

**Figure 6.2** shows the compaction of HMA mix in the mold using a hand driven vibratory compactor. A constant spray of water on the compactor surface is required to prevent materials sticking to the roller surface during compaction. The frequency and amplitude of vibration of the compactor can be adjusted.



Figure 6.2: Compaction of HMA in the mold using vibratory compactor

The mold for building the layered pavement is also shown in **Figure 6.2** where the top surface of top layer HMA is visible. A typical cross section of the test beds inside the mold is shown in **Figure 6.3**.

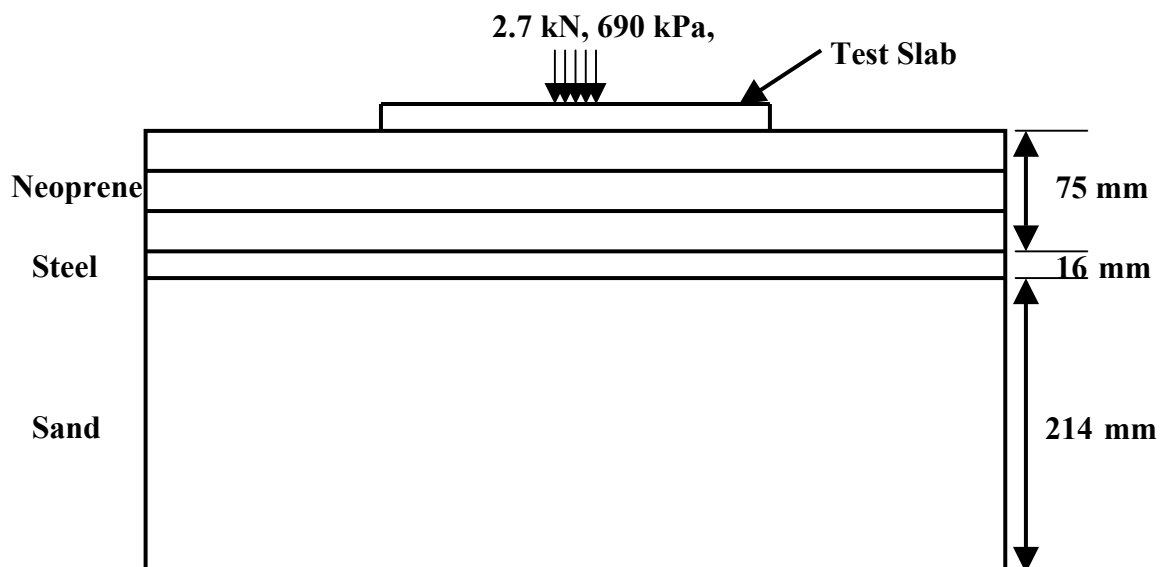


Figure 6.3: Typical cross section of model pavement

As shown in **Figure 6.3**, a typical test section consists of three layers of 25 mm thick Neoprene sheets followed by a 16 mm thick steel plate and a 214 mm thick sand layer. The factors behind consideration of these materials are presented in **Chapter 9**. The typical load is a 2.7 kN wheel load with 690 kPa tire pressure.

### **(3) The Environment Chamber**

Fatigue tests were carried out at different temperatures and during the test a constant temperature was required. The environment chamber of MMLS3 was used for this purpose. The environment chamber is a cover on top of the test bed. It has one inlet to blow cold air inside the chamber and an outlet to blow out the air so that a constant flow of cold air on top of the pavement is maintained. The temperature is controlled by a unit where a particular temperature can be preset before start of a test. The unit blows the cold air for certain time until the temperature reaches slightly below the target value and then stops. It is automatically restarted when the temperature crosses the target value and this cycles goes on for the whole test period.

### **6.3 Aggregates**

Following are the specifications of aggregates used in making HMA:

- Nominal Maximum Aggregate Size: 9.5 mm
- CA Angularity (ASTM D5821): 98.6/98.2
- Fine Aggregate Angularity (AASHTO T304): 47
- Sand Equivalent (AASHTO T176): 73
- Washington Degradation (Maine DOT): 75
- Combined Aggregate Bulk Specific Gravity: 2.687

The gradation of the aggregates is shown in **Table 6.1**.

Table 6.1: Gradation of aggregates used

Sieve Size		% Passing
(inch)	(mm)	
1/2	12.5	100
3/8	9.5	95
4	4.75	60
8	2.36	47
16	1.18	33
30	0.6	20
50	0.3	12
100	0.15	8
200	0.075	5

#### 6.4 Asphalt

The specifications for the asphalt binder used for preparation of HMA is:

- Grade: PG 64-28
- Percent binder: 5.9%

#### 6.5 Steel

Hot rolled 16 mm thick steel plate was used.

#### 6.6 Neoprene

Grade 80 neoprene was used in the tests. Initially D60 grade was used for trial slabs, later D80 was used as standard practice.

## Chapter 7

# TEST METHODS USED IN THIS STUDY OTHER THAN APT

### 7.1 Introduction

As mentioned earlier in this thesis, one of the objectives of this study was to develop a test protocol for using the MMLS3 as a scaled model for fatigue characterization of HMA in the laboratory. Fatigue characteristics of HMA are dependent on several other material characteristics of HMA, such as resilient modulus and creep compliance. Therefore, it was also necessary in this study to measure these properties of the mix. Both of these material properties were measured in indirect tensile mode. The theory and the methods are discussed in the following sections.

### 7.2 Indirect Tensile Test (ITT)

In the Indirect Tensile Test (ITT) a load is applied diametrically to a cylindrical sample of HMA. **Figure 7.1** shows the general setup of the test where a load of magnitude  $F$  is acting along the diameter of a sample of thickness (height)  $h$  and diameter  $d$ . The load is distributed over the length  $w$  on the thickness of the sample.

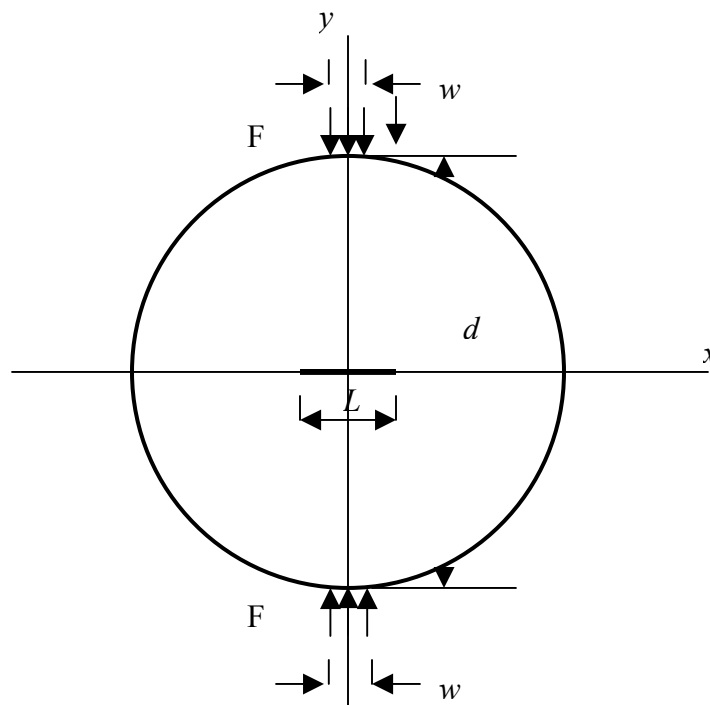


Figure 7.1: Indirect Tensile Test

In **Figure 7.1**,  $L$  indicates the length of a section of horizontal diameter of the sample and  $x$  and  $y$  are the Cartesian coordinate axes. During the test for the resilient modulus,  $F$  is the magnitude of a load with certain period and rest time. The response measured during the resilient modulus test is the total deformation of horizontal axes. During the creep compliance test,  $F$  is a constant step load and the response measured is the strain along the portion  $L$  of diameter using a strain gauge of length  $L$ . Therefore, before starting the discussion of each test method and calculations, it will be useful to present the general equations for calculations of strain, since same setup is used for testing both creep compliance and resilient modulus of HMA.

### 7.2.1 Calculation of Strain

The calculation of strain is based on the assumption of plane stress behavior [27]. Under this assumption, the strain at any location along horizontal diameter,  $\varepsilon_x(x)$ , is given by:

$$\begin{aligned}
a &= R \cos \alpha \\
b &= x - R \cos \alpha \\
c &= (a^2 + b^2)^2 \\
\sigma_x(x) &= -\frac{4P}{\pi} \frac{ab^2}{c} + \frac{P}{\pi R} \cos \alpha \\
\sigma_y(x) &= -\frac{4P}{\pi} \frac{a^3}{c} + \frac{P}{\pi R} \cos \alpha \\
\varepsilon_x(x) &= \frac{1}{E} (\sigma_x(x) - \nu \sigma_y(x)) \\
P &= \frac{F_0}{wh} \frac{d}{2} d\alpha
\end{aligned} \tag{7.1}$$

where,  $x$  is any position along horizontal diameter along which the strain is being measured,  $F_0$  is the constant load acting along vertical diameter and distributed over the length  $w$  across the height  $h$ ,  $E$  and  $\nu$  are the Young's modulus and Poisson's ratio of HMA respectively,  $L$  is the length of strain gauge,  $R$  is the radius of cylindrical sample,  $\theta$  is half of the angle created at center of the disk by the width  $w$  of the load and  $\alpha$  is the angle created between vertical diameter and the arc corresponding to position  $x$  along horizontal diameter.

Stresses and strain can thus be found at any point inside the disk by performing the above integrations. Numerical integrations can be performed for the above relations and the stress and strain distributions along the vertical and horizontal diameter can be obtained by choosing appropriate values of  $x$  and  $y$ . When strain is required to be computed over a certain length,  $L$ , along the horizontal diameter (as often done with using foil strain gauges glued to the surface along the horizontal diameter), the average strain over the length  $L$  can be obtained as:

$$\varepsilon_{av} = \frac{1}{L} \int_{-L/2}^{L/2} \varepsilon_x(x) dx \tag{7.2}$$

### 7.3 Resilient Modulus Test

After the completion of loading of each test slab with the MMLS3, cores were taken from inside and outside the wheel path and resilient moduli of the cores were determined in the

ITT mode. The sample was placed under a diametrical repeated loading equipment (Universal Testing Machine) with Linear Variable Displacement Transducers (LVDTs) placed on both sides of the horizontal diameter to measure horizontal deformations. **Figure 7.2** shows a sample of HMA in resilient modulus test setup along with a strain gauge attached with this sample. In **Figure 7.2** the LVDTs can be noted fixed along the diameter and the loading is applied on top through a horizontal metal bar and the sample is rested at bottom on a similar bar. The horizontal bar provided the distributed load along the edge of the sample.

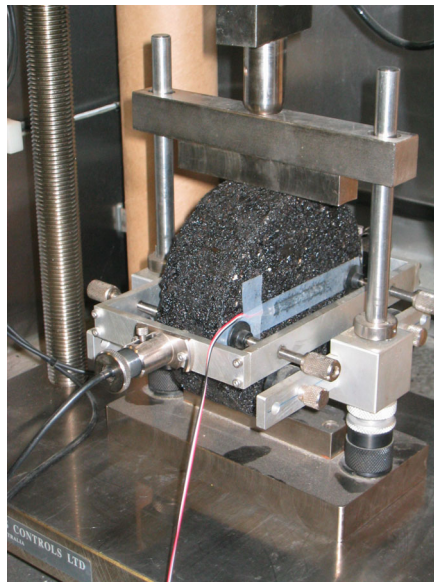


Figure 7.2: Resilient Modulus Test Setup

### 7.3.1 The Loading

The load used for resilient modulus test was a periodic load with rest time between periods. The general pattern of periodic load is show in **Figure 7.3**.

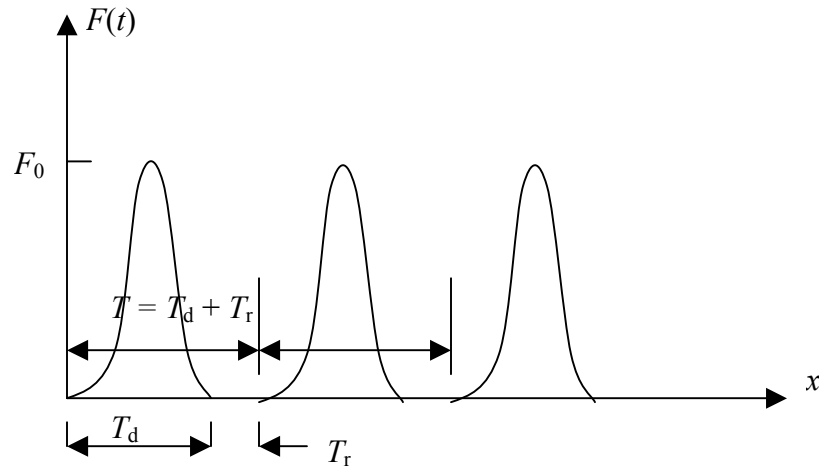


Figure 7.3: Periodic Loading for Resilient Modulus Test

In **Figure 7.3**,  $T_d$  and  $T_r$  represents the loading duration and rest time respectively.  $T$  is the period of loading and  $F_0$  is the magnitude of loading.

### 7.3.2 Calculation of Resilient Modulus

By performing the integration in Eq. 7.2 over the whole diameter ( $L=d$ ) and assuming the load  $F$  as a point load, the elastic modulus (resilient modulus) can be obtained as shown in Equation 5.4.

### 7.4 Creep Test

Creep tests were performed on samples cored from the test slabs to determine creep compliance,  $J(t)$ . The samples were divided into groups of similar voids and tested under static creep loading in ITT mode. The setup was similar to that shown in **Figure 7.2**. A foil strain gauge was fixed along the diameter normal to loading diameter of each sample tested. A typical loading duration was 1800 seconds. The data acquisition system used for MMLS3 testing was used to perform continuous data acquisition. The acquired data were post processed to calculate  $J(t)$ .

#### 7.4.1 Calculation of Creep Compliance, $J(t)$

The creep strains,  $\varepsilon(t)$ , were converted to creep compliance,  $J(t)$ , using the following relation:  $\varepsilon(t) = AF_0J(t)$ , where  $A$  is a factor depending on geometry of the sample and  $F_0$  is the static load. The factor  $A$  is given as:

$$\begin{aligned}
 a &= R \cos \alpha \\
 b &= x - R \cos \alpha \\
 c &= (a^2 + b^2)^2 \\
 \sigma_x(x, t) &= -\frac{4P(t)}{\pi} \frac{ab^2}{c} + \frac{P(t)}{\pi R} \cos \alpha \\
 \sigma_y(x, t) &= -\frac{4P(t)}{\pi} \frac{a^3}{c} + \frac{P(t)}{\pi R} \cos \alpha \\
 \varepsilon_x(x, t) &= \frac{1}{E} (\sigma_x(x, t) - \nu \sigma_y(x, t)) \\
 P(t) &= \frac{F_0}{wh} \frac{d}{2} d\alpha \\
 A &= \frac{E}{LF_0} \int_{-L/2}^{L/2} \int_{-\theta}^{\theta} \varepsilon_x(x, t) dx d\alpha \\
 \theta &= \frac{w}{2R}
 \end{aligned} \tag{7.3}$$

where,  $x$  is any position along horizontal diameter along which the strain is being measured,  $F_0$  is the constant load acting along vertical diameter and distributed over length  $w$  across the height  $h$ ,  $E$  and  $\nu$  are the Young's modulus and Poisson's ratio of HMA respectively,  $L$  is the length of strain gauge,  $R$  is the radius of cylindrical sample,  $\theta$  is half of the angle created at center of the disk by the width  $w$  of the load and  $\alpha$  is the angle created between vertical diameter and the arc corresponding to position  $x$  along horizontal diameter.

## Chapter 8

# TEST AND ANALYSIS PLAN

### 8.1 Introduction

It was decided to test HMA slabs with different thickness/foundations under similar loading and temperature, such that different initial strain levels were achieved. Using different grades (D60 and D80) and different numbers of 25 mm thick neoprene sheets, different foundation properties were obtained. The fatigue response (i.e. tensile strain, deterioration of modulus and cracking) corresponding to initial strain levels was then determined. Data from tests of nine slabs, referred to as Slab J, K, L, N, P, Q, R, S and T are discussed in the following sections. Slabs A through I were used to determine proper slab preparation, setup and the effect of speed on strains. An average temperature of 20°C was targeted for all slabs tested. The vertical profile for Slab J, K and L consisted of, from top to bottom, HMA slab of variable thickness, three 25 mm thick neoprene sheet layers of grade D80 (the top layer tacked with RS-1 asphalt emulsion), one 16 mm thick steel plate and 214 mm thick sand layer. For slab N, an additional neoprene layer of thickness 25 mm and grade of D60 grade was placed over the two existing layers to reduce the stiffness of the support. Slab P and Q were placed on four neoprene layers (three D80 and one D60). Four longitudinal and four transverse strain gauges were fixed to the bottom of each test slab. Surface profiles were obtained using profilometer at several intervals during each test by stopping the MMLS3. Cores were obtained from each test slab from both inside wheel path and outside wheel path after the completion of loading. At the end of each test, entire strain, thermocouple and surface profile data were analyzed for determination of fatigue failure points and rutting.

### 8.2 Test Plan

A schematic diagram of overall test and analysis plan is shown in **Figure 8.1**.

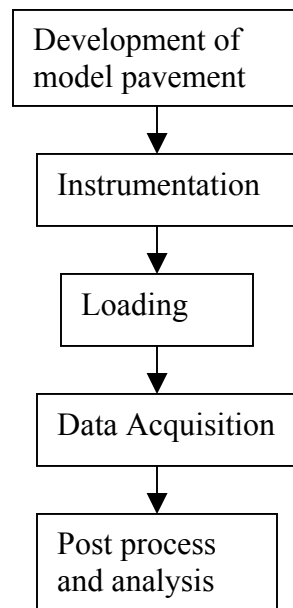


Figure 8.1: Test and Analysis Plan

The test plan consists of development of a model pavement, instrumentation, loading and data acquisition. The development of the model pavement and test protocol, loading and data acquisition are discussed in detail in **Chapter 9**. The general instrumentation of test slabs is discussed below.

### 8.2.1 Instrumentation

As discussed in Chapter 4 as part of the literature review, proper instrumentation and continuous data acquisition is necessary for monitoring the fatigue behavior throughout the duration of the test. To achieve this, strain gauges and thermocouples were fixed at the bottom of the test slabs. Four longitudinal and four transverse strain gauges were used for each test slab for continuous measurement of strain. Four thermocouples were used for each test slab for continuous measurement of temperature. The general positions of strain gauges and thermocouples are shown in the schematic diagram in **Figure 8.2**.

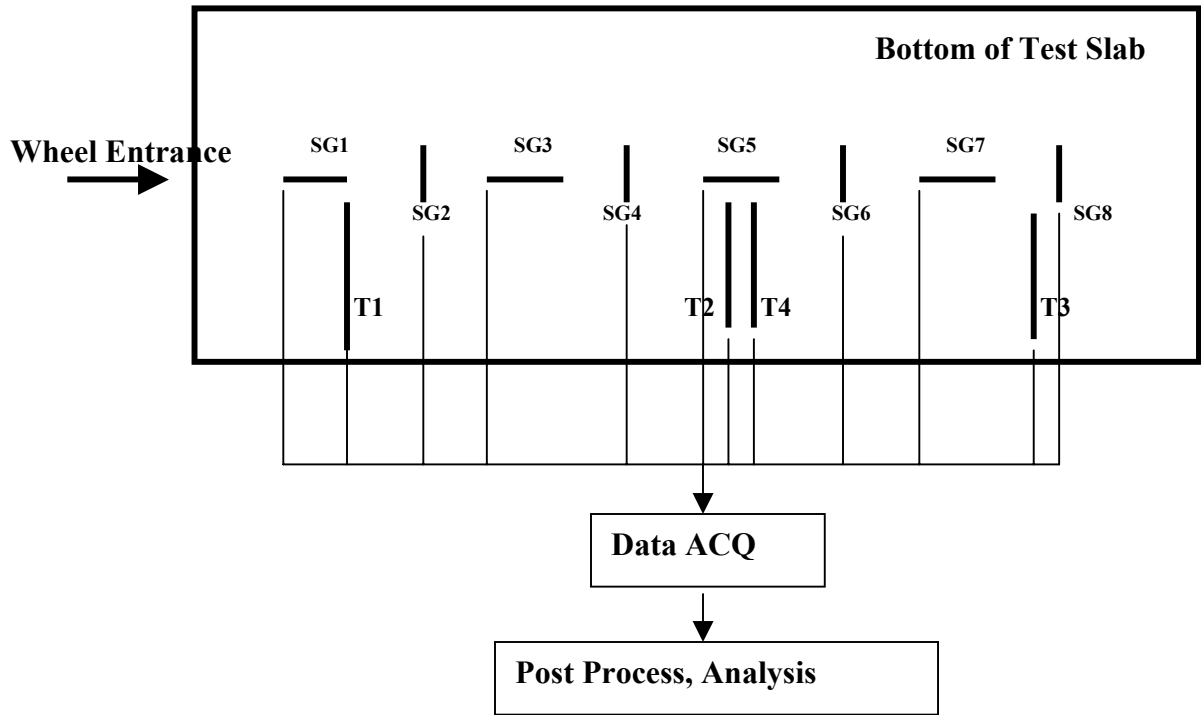


Figure 8.2: Positions of Strain Gauges and Thermocouples

In **Figure 8.2**, SG1 through SG8 indicate the strain gauges, among which odd numbers are positioned along the direction of wheel movement (longitudinal) and even numbers were placed normal to the direction of wheel movement (transverse). T1 through T4 are thermocouples. The thin lines indicate the wires connecting the strain gauges and thermocouples to the data acquisition system.

### 8.3 Analysis Plan

Following are the steps of analysis and post processing of data presented in this thesis.

- Calculation of resilient strain history
- Calculation of permanent strain history
- Determination of failure strain
- Determination of failure load corresponding to failure strain
- Determination of stiffness reduction due to traffic

- Analysis of model pavement using finite element
- Observation of cracks and effect of loading on formation of crack length
- Observation of effects of factors affecting fatigue behavior of HMA
- Development of characteristic curves showing relation between initial strain and failure load
- Comparison between MMLS3 fatigue curves and curves obtained using other standard methods
- Development of analytical model of MMLS3 model pavement under moving wheel load

## Chapter 9

# DEVELOPMENT OF MODEL PAVEMENT AND TEST PROTOCOL USING MMLS3

### 9.1 Introduction

In this section, a detailed discussion is presented on slab preparation and testing procedures that were developed at Worcester Polytechnic Institute (WPI) and used in this study. Each step of the process is presented in separate subsections. The steps are presented in the same sequence in which they are performed during the building and testing of a scaled pavement structure. A schematic diagram of the different steps are shown in **Figure 9.1**.

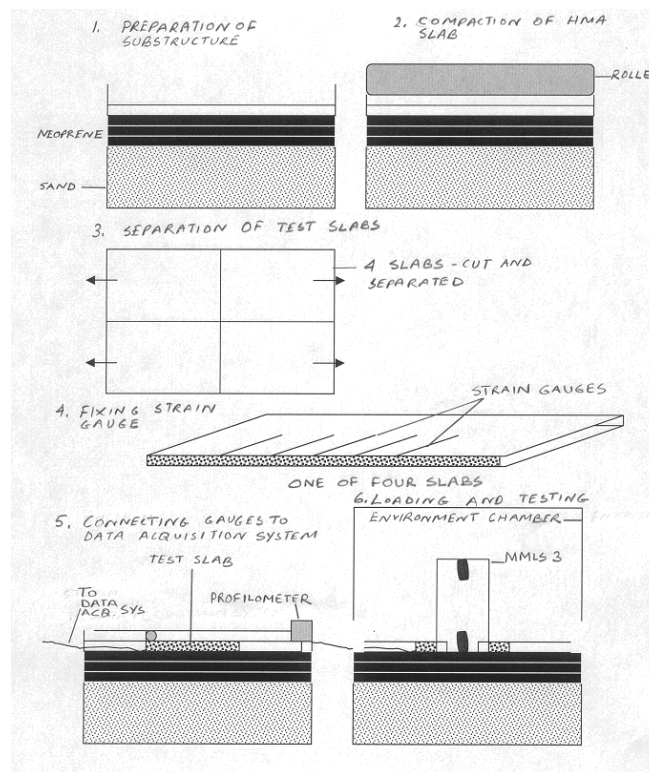


Figure 9.1: Schematic diagram of steps

## 9.2 Preparation of the substructure and compaction platform in the mold

Since the objective of this study is to investigate the fatigue response under the surface layer, a substructure with low rutting potential was necessary to minimize rutting. Also, a firm and level surface was necessary to use as compaction platform such that slabs can be easily separated from the platform. A frame with adequate height was also needed to put down the mix before compaction.

In order to build a scaled model of an actual flexible pavement, one needs to use granular materials at the bottom and bound material layers at the top. Natural sand used for making concrete was used for filling the bottom 300 mm of the mold. First the sand was made to workable moisture content to facilitate compaction. Then a vibratory roller was used to compact the sand. A 12.5 mm thick steel plate and a 25 mm thick Neoprene sheet was placed on top of the sand and compaction was done on top of the Neoprene sheet without the vibratory mode. After the compaction of the sand, the neoprene layer and steel plate were removed. A Geogauge (which determines the stiffness of underlying material and the modulus is calculated from the stiffness) was used to measure the modulus of the compacted sand. The results of Geogauge reading are shown in **Table 9.1**.

Table 9.1: Calculation of Young's modulus of sand (using Geogauge)

Measured Stiffness, K MN/m	Young's Modulus $E = \frac{K(1-\nu^2)}{1.77R}$ MPa
5.35	42.2
4.36	34.4
4.24	33.4
4.17	32.9
4.21	33.2
4.66	36.7
4.35	34.3
4.26	33.6
Average=	35.1

In **Table 9.1**,  $\nu$  = Poisson's ratio of sand = 0.40 (assumed), R = Outside radius of ring foot = 57.15 mm and K=stiffness. To minimize rutting in the subsurface layers, it was

decided to use three 25 mm thick Neoprene layers (D60). Since the mold not only serves as the container for the scaled pavement structure, but also as the platform for compacting the slabs, the steel plate was intended to be placed on top of the Neoprene layers to prepare the compaction platform of the HMA. Some sand was removed and the sand was re-leveled in order to have sufficient gap to accommodate 75 mm of rubber and the 12.5 mm thick the steel plate. A wood board of 87.5 mm wedge height was used to level the sand. The level of the sand was carefully monitored to make sure that it was exactly 87.5 mm free from the sand to the top of the mold. **Figure 9.2** shows the leveled sand surface.



Figure 9.2: Leveled surface of sand

Next, three layers of Neoprene, each 2742 mm long and 915 mm wide covering whole surface area of mold, were placed on the sand. The Neoprene layers were tacked with RS-1 asphalt emulsion. There were 50 mm gaps on either end, which were filled with sand. **Figure 9.3** shows how the setup looked after the gaps were filled in the sides with sand.



Figure 9.3: Compaction platform with neoprene layer for trial slab

The steel plate, intended to be compaction platform, was lowered carefully (**Figure 9.4**) on to the mold to prevent any warping. However, slight warping of the plate was noted due to its self-weight and it was left over the weekend on the mold with some weight on it to straighten it out. A wood frame was constructed all around the mold to facilitate compaction (**Figure 9.5**).



Figure 9.4: Lowering the steel plate



Figure 9.5: Steel compaction platform with wooden frame

At the end of compaction of the first set of slabs, while removing the smaller slabs after cutting, a significant amount of effort was needed to separate the slabs from the steel plate. The amount of effort needed was thought to be damaging the slabs. In a subsequent trial, a better approach was developed and used. Four pieces (four pieces for four slabs) of normal roofing aluminum (1 mm thick) flashing were placed on the steel plate (**Figure 9.6**) to facilitate separation of slab from steel plate. A large piece of flashing was cut into four pieces (corresponding to the four HMA slabs) and the edges of the flashings were smoothed out. These sheets were treated with a silicone spray before compaction.



Figure 9.6: Aluminum sheets to be placed on top of the steel plate

After compaction, the HMA slabs were removed with the aluminum flashing at the bottom. The slabs were placed in wooden boards, and after cooling down to 4°C, the aluminum flashing was peeled off the HMA slabs without any problem (**Figure 9.7**).



Figure 9.7: Aluminum sheets were peeled off from bottom of test slab

Next, on close examination a few spots in the HMA slab were noted which showed “blow ups”, most possibly due to curling up of the aluminum sheet due to change

in temperature. In the next trial, it was decided to use laminated plywood boards. These plywood boards were stiff enough to be placed directly on the Neoprene, thus eliminating the need for placing the steel plate on top of the mold for compaction and removing it later on. An asphalt roofing paper was placed on plywood board prior to laydown of mix, to facilitate easy separation of the slab from the plywood boards. After compaction, the slabs were cut and no curling or other damage of slab was observed and hence, this method was adopted as standard practice for all subsequent slabs.

### **9.3 Preparation of mix**

In this step, the challenge was to produce enough mix to produce a HMA slab at least 25 mm thick. This necessitated a mix amount of at least 150 kg. Overnight, batches of 15 kg each were prepared with representative aggregates and kept in buckets in an oven maintained at mix temperature. About four hours before mixing, hot (sufficient to be poured easily) asphalt was poured into the asphalt container of a Wirtgen [28] foamed asphalt producing equipment (an equipment used for dispensing heated asphalt during the production of foamed asphalt – in this case used to produce normal asphalt). Asphalt was heated up to 150<sup>0</sup>C in the foamed asphalt plant before mixing with the aggregate. The mixes were placed in an oven for short-term aging. Part of the mix was used for determination of theoretical maximum densities. The amount of mix required for laydown was determined with the help of a spreadsheet, which was also used during the laying down process to keep track of the actual amount laid down and the amount needed. The target density was 92 to 94 percent of theoretical maximum density.

### **9.4 Set up before laydown and compaction of mix**

Radiant heaters [29] were used for heating up the compaction platform as well as for keeping the mix hot during laydown and compaction (Figure 9.8). The heaters were placed at 375 mm above the surface to cover a wider area and have more uniform heating. The compaction platform was sprayed with the silicone spray just before

laydown. The heaters did help in maintaining sufficiently high mix temperature, which facilitated compaction.



Figure 9.8: Heaters on top of compaction platform

### 9.5 Laydown of mix

The compaction surface was sprayed with silicone spray [30] (**Figure 9.9**). A spreadsheet was developed and used for estimating the amount of mix required for producing a slab of specific thickness. A typical spreadsheet is shown in **Figure 9.10**. The mix needed to be laid down uniformly across the width and along the length and evened out with spade to reduce segregation. In first trial, segregation was noted. In subsequent trials, the placement of mix was done at several spots instead of one place and a scraper was used to redistribute the aggregates to minimize segregation.



## 9.6 Compaction of mix

A paint sprayer was used to spray water on the drum during rolling. It was observed that thickness of slabs were uniform with little curling up on corners and sides. The curled portions were cut out before cutting different slabs. **Figure 9.11** shows the compaction of mix in the mold.



Figure 9.11: Compaction of HMA in the mold

## 9.7 Checking density with a non-nuclear density gauge

Densities of initial trial compacted slabs were determined using a non-nuclear density gauge (Pavement Quality Indicator, PQI) to get an indication of the degree of compaction. Readings were taken at around each core location (**Figure 9.12**). Bulk specific gravity and resilient modulus values were also determined for each slab, for un-trafficked and trafficked areas.



Figure 9.12: PQI readings are being taken on top of the compacted slab

### 9.8 Conditioning slab before cutting

To prevent the slabs from any stress-induced damage during cutting and detaching from compaction platform, the slabs needed to be cold enough to have a high stiffness. For initial trial slabs, the environment chamber of MMLS3 was used to cool the compacted mix inside mold before cutting. The chamber was placed, and the air conditioning unit was started to drop the temperature down to 3°C to allow for cutting the trial slab. However, the lip of the blower was off the trial slab by one-third and the thermocouple was placed at the other ends, as a result, a significant amount of cold air was wasted and the slab cooled down from 21°C to 17°C in three hours. At the front of the lip the temperature was 9°C and at the thermocouple region it was 17°C. Also, the lip was slightly higher than the surface of the slab. It was decided to place the lips adjacent to the trial slab and the environmental chamber was placed on insulation and the hole for the blower lips were sealed with insulation. The lips were placed adjacent to the trial slab (at the far end of the mold). The air conditioning unit was operated for 4.5 hours and the temperature of the pavement (surface) dropped from 23°C to 9°C. A better method to cool down the slab for cutting was sought. Dry ice was obtained and placed on the slab (in bags). The temperature went down to 0°C within 5-7 minutes. At that point the ice

was removed and cutting started. This method was adopted as the standard procedure for all subsequent slabs tested.

### 9.9 Cutting the compacted slab

A masonry cutoff blade was used initially to cut the slabs but was later replaced by a diamond tooth blade to prevent it from wearing out. First, a small strip along all four sides was cut off to get rid of the warped edges. During cutting, water was used to prevent dust generation and possible clogging of the HMA pores. Next, cutting was done along the length through the centerline of the slab and then along the width, dividing the whole slab into four pieces of equal size (1295 mm long and 465 mm wide). A beveled edged wedge was inserted in the cut centerline by tapping with a hammer. A metal meter scale was inserted sideways inside one side of the slab. A wood beam was used to hit one side of the slab, gently, until after five minutes when one part became loose and could be slid off onto a wood board. Prior to this step, ice bags filled with water ice/snow were placed on top of the HMA surface until the temperature went down to 0°C. **Figure 9.13, 9.14, 9.15 and 9.16** show the whole process of cutting and removing slabs.



Figure 9.13: Cutting of slab after cooling by dry ice (note dry ice bags on top of adjacent slabs)



Figure 9.14: Separating slabs.



Figure 9.15: Sliding slab onto plywood board.



Figure 9.16: Removing plywood board.

### 9.10 Handling cut and separated slabs

Slabs were cooled down to 0-4°C and a plywood board was placed on top of the slab. With another plywood board already at the bottom of the slab, the whole thing was flipped over. No visible sign of distortion or crack was observed. Next, temperature of the slab was brought back to room temperature (approximately 20°C – 25°C).

### 9.11 Selecting strain gauges

Although a number of different types of strain gauges are available, a specific type was sought that would provide data in the expected range and load repetitions as well as thin enough to be put into grooves in thin pavement layers (25 to 40 mm thick) planned for testing. The N2A-Series model of 120-ohm foil gauges was found to be most suitable for this purpose.

### **9.12 Putting molds for housing the strain gauges**

To determine strains at the bottom of HMA slab, it was decided to use strain gauges as close to the bottom surface as possible. Initially shims were glued to the compaction platform to make impression underside of the slab, where strain gauges were later glued to the slab. This whole arrangement was done to put the strain gauges slightly inside the underside of the slab and prevent touching the top of the Neoprene layer. The first exercise was to determine the shim of the right thickness – one that would leave enough room for placing the strain gauges but would not leave a big gap, which needs to be filled. Impressions left by shims of different thickness – 0.254, 0.508, 0.762, 1.016, 1.27 and 1.524 mm thick, as well as impression left by the wires and a 6.35 mm diameter rod (for the air conditioning unit thermocouple) were checked in a trial slab. Considering the thickness of the selected strain gauges, the shim with the 1.524 mm thickness was found to be the best. The length of the shim was selected to be to be little greater than the length of foils strain gauges to accommodate soldering with wires.

In working with a trial slab, a different method, using a diamond blade saw cutting tool was found to be better suited for creating the impressions for housing the strain gauges and thermocouples. This could be done after the slab is compacted, cut and removed from the mold and before it is put down in the mold for loading and testing. This eliminated the tedious task of gluing down shims to compaction platform before compaction. This also provided a much smoother surface on which the strain gauge can be attached.

### **9.13 Attaching strain gauges**

Initially a glue needing three days of curing was used as suggested by the manufacturer of the strain gauges. Later a two-part quickset epoxy (“High strength five minute epoxy”) was found to be adequate for producing good bond within five minutes. Asphalt binder was used to fill the grooves below and beside the strain gauge. Short wires were soldered to the strain gauges. Once inside, the sticky tapes were removed from the (curing) strain gauges. Four transverse and four longitudinal strain gauges and four thermocouples were

used for test slabs. **Figure 9.17** shows cutting grooves for strain gauges and **Figure 9.18** shows the process of fixing and wiring strain gauges.



Figure 9.17: Cutting grooves for strain gauges and thermocouples



Figure 9.18: Attaching strain gauges

#### **9.14 Setup for housing and restraining the test pavement slab for loading and testing and profiling slab prior to loading**

The test slab was restrained all around by using concrete slabs made of quickset premix concrete. This was done to create a better confinement of the test pavement slab and minimize any movement. It took approximately two to three hours to cure the concrete sufficiently. The profilometer was used prior to loading to determine surface profiles. Profiles were determined to estimate rutting, as well as to obtain data for identifying the contribution of consolidation and shear flow towards rutting. The profilometer was used to measure surface profile at shorter intervals of loading initially and also at longer interval at later stages of loading, when rutting did not increase significantly.

#### **9.15 Checking strain gauges, data acquisition system**

For proper data acquisition (from strain gauges and thermocouples), it was necessary to make sure that the strain gauges as well as the data acquisition system were working properly. One critical point was to determine if there was any significant “noise” from surrounding electrical devices, and if there was, how to cancel their effects through the use of proper filters. Strain gauge readings were checked against predicted strains from cores tested in the indirect tensile mode. The gauges were calibrated using an aluminum beam of known properties and load. Signals from strain gauges were checked by running the MMLS3 at different speeds. The effects of noise were checked by acquiring data without running the MMLS3 and with running the MMLS3 and comparing the results. A National Instruments® (NI) data acquisition system with Labview® software was selected for basic data acquisition system after initial trials with different systems, software and improvised low pass filters. It has been observed that NI acquisition systems with inbuilt low pass filter eliminated the noise successfully. Later MATLAB® 6.5/R12 was used for post processing data.

### 9.16 Making MMLS3 ready for test

The tires were pumped up to 690 kPa and the pressure was checked using a pressure gauge. Grooves were cut through the wood boards so that the wires from the strain gauges can be taken out without pinching them. The wires were stripped so that the wires do not stick out of the groove. **Figure 9.19** shows the complete setup before starting loading. The loading was stopped at certain intervals during each test and the pavement was checked for profiles and cracks.



Figure 9.19: Complete setup before starting loading